Chapter 1

τ decays into hadrons

The principal input to our QCD analysis are measurements of τ-decays, which represent an excellent tool to access low energy QCD.

The τ-particle is an elementary particle with negative electric charge and a spin of 1/2. Together with the lighter electron and muon it forms the *charged Leptons*[1]. Even though it is an elementary particle it decays via the *weak interaction* with a lifetime of $\tau_\tau = 2.9 \times 10^{-13}$ s and has a mass of 1776.86(12) MeV[**PDG2018**]. It is furthermore the only lepton massive enough to decay into Hadrons. The final states of a decay are limited by *conservation laws*. In case of a τ-decay they must conserve the electric charge (-1) and *invariant mass* of the system. Thus, as we can see from the corresponding Feynman diagram (see fig. 1.1)[2] the τ decays by the emission of a *W boson* and a tau-neutrino ν_τ into pairs of $(e^-, \bar{\nu}_e), (\mu^-, \bar{\nu}_\mu)$ or $(q, \bar{q})$.
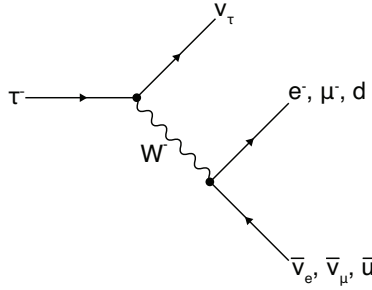

Figure 1.1: Feynman diagram of common decay of a τ-lepton into pairs of lepton-antineutrino or quark-antiquark by the emission of a *W boson*.

The hadronic $\tau - decay$ provides one of the most precise ways to determine the strong coupling [**Pich2016**] and can be calculated to high precision within

---

[1]Leptons do not interact via the strong force.

[2]The τ-particle can also decay into strange quarks or charm quarks, but these decays are rather uncommon due to the heavy masses of s and c.

the framework of QCD.

begin old The τ-lepton is the only lepton heavy enough to decay into Hadrons. It permits one of the most precise determinations of the strong coupling α_s. The inclusive τ-decay ratio

$$R_\tau = \frac{\Gamma(\tau \to \nu_\tau + \text{Hadrons})}{\Gamma(\tau \to \nu_\tau e^+ e^-)} \tag{1.1}$$

can be precisely calculated and is sensitive to α_s. Due to low the mass of the τ-lepton $m_\tau \approx 1.8\,\text{GeV}$ τ-decays are excellent for performing a low-energy QCD analysis. The theoretical expression of the hadronic τ-decay ratio was first derived by [**Tsai1971**], using current algebra, a more recent derivation making use of the *optical theorem* can be taken from [**Schwab2002**]. The inclusive ratio is then given by:

$$R_\tau(s) = 12\pi \int_0^{m_\tau} = \frac{\mathrm{d}s}{m_\tau^2}\left(1 - \frac{s}{m_\tau^2}\right)\left[\left(1 + 2\frac{s}{m_\tau^2}\right)\operatorname{Im}\Pi^{(T)}(s) + \operatorname{Im}\Pi^{(L)}(s)\right], \tag{1.2}$$

where $\operatorname{Im}\Pi$ is the two-point function (see **??**). In the case of τ-decays we only have to consider vector (V) and axial-vector contributions (A) of decays into up, down and strange quarks. Thus taking i,j as the flavour indices for the light quarks (u, d and s) we can express the correlator as

$$\Pi^{V/A}_{\mu\nu,ij}(s) \equiv i \int \mathrm{d}x\, e^{ipx} \langle\Omega|T\{J^{V/A}_{\mu,ij}(x)J^{V/A}_{\nu,ij}(0)^\dagger\}|\Omega\rangle, \tag{1.3}$$

with $|\Omega\rangle$ being the physical vacuum. The vector and axial-vector currents are then distinguished by the corresponding dirac-matrices (γ_μ and $\gamma_\mu\gamma_5$) given by

$$J^V_{\mu,ij}(x) = \overline{q}_j(x)\gamma_\mu q_i(x) \quad \text{and} \quad J^A_{\mu,ij}(x) = \overline{q}_j(x)\gamma_\mu\gamma_5 q_i(x). \tag{1.4}$$

The two-point function can be decomposed into its vector and axial-vector contributions, but also into transversal and longitudinal components. We will give now both of these decompositions and relate them, which has some implications for a common used approximation: the **chiral limit**, where the quark masses are taken to 0 ($m_q \to 0$).

Starting with the decomposition into vector, axial-vector, scalar (S) and pseudo-scalar (P) components we can write [**Broadhurst1981**, **Jamin1992**]

$$\Pi^{\mu\nu}(q^2) = (q^\mu q^\nu - q^2 g^{\mu\nu})\Pi^{V,A}(q^2) + \frac{g^{\mu\nu}}{q^2}(m_i \mp m_j)\Pi^{S,P}(q^2)$$
$$+ g^{\mu\nu}\frac{(m_i \mp m_j)}{q^2}[\langle\overline{q}_i q_i\rangle \mp \langle\overline{q}_j q_j\rangle], \tag{1.5}$$

which is composed of a vector $\Pi^{V,A}$ and scalar $\Pi^{S,P}$ part. The third term are corrections arising due to the physical vacuum $|\Omega\rangle$. The latter decomposition rewrites the correlator $\Pi^{\mu\nu}(q^2)$ into transversal and longitudinal components:

$$\Pi^{\mu\nu}(q^2) = (q^\mu q^\nu - g^{\mu\nu}q^2)\Pi^{(T)}(q^2) + q^\mu q^\nu \Pi^{(L)}(q^2). \tag{1.6}$$

With the two decompositions eq. (1.5) and eq. (1.6) we can now identify the longitudinal components of the correlator as being purely scalar, by multiplying eq. (1.5) by two four-momenta and making use of the Ward-idendity **??** we can write

$$q_\mu q_\nu \Pi^{\mu\nu}(q^2) = (m_i \mp m_j)^2 \Pi^{S,P}(q^2) + (m_i \mp m_j)[\langle \bar{q}_i q_i \rangle \mp \langle \bar{q}_j q_j \rangle], \qquad (1.7)$$

which then can be related to the longitudinal component of eq. (1.6) by comparisson of the two equations

$$q_\mu q_\nu \Pi^{\mu\nu}(q^2) = q^4 \Pi^{(L)}(q^2) = s^2 \Pi^{(L)}(s) \quad \text{with} \quad s \equiv q^2. \qquad (1.8)$$

In a more eloquent way this can be expressed as

$$s^2 \Pi^{(L)}(s) = (m_i \mp m_j)^2 \Pi^{(S,P)}(s) + (m_i \mp m_j)[\langle \bar{q}_i q_i \rangle \mp \langle \bar{q}_j q_j \rangle], \qquad (1.9)$$

where we can see, that all mass terms are related to the longitudinal component of the correlator. By defining a combination of the transversal and longitudinal correlator

$$\Pi^{(T+L)}(s) \equiv \Pi^{(T)}(s) + \Pi^{(L)}(s) \qquad (1.10)$$

we can additionaly relate the transversal and vectorial components via

$$\Pi^{\mu\nu}(s) = \underbrace{(q^\mu q^\nu - g^{\mu\nu} q^2)\Pi^{(T)}(s) + (q^\mu q^\nu - g^{\mu\nu} q^2)\Pi^{(L)}(s)}_{=(q^\mu q^\nu - g^{\mu\nu} q^2)\Pi^{(T+L)}(s)} + \frac{g^{\mu\nu} s^2}{q^2}\Pi^{(L)}(s),$$

$$(1.11)$$

such that

$$\Pi^{(V,A)}(s) = \Pi^{(T)}(s) + \Pi^{(L)} = \Pi^{(T+L)}, \qquad (1.12)$$

where the vector/ axial-vector component of the correlator is now related to the newly defined transversal and longitudinal combination of the correlator. As the τ-decays, with the limiting factor of the τ-mass, can only decay into light quarks we will often neglect the quark masses and work in the so called chiral limit. In the chiral limit the longitudinal component, which is proportional to the quark masses, of the correlator vanishes.

Examining the inclusive ratio R_τ in eq. (1.1), we note that we have to deal with a problematic integral over the real axis of $\Pi(s)$ from 0 up to m_τ. The integral is problematic for two reasons:

- **Perturbative Quantum Chromodynamcs** (pQCD) and the OPE breaks down for low energies (over which we have to integrate).

- The positive euclidean axis of $\Pi(s)$ has a discontinuity cut and can theoretically not be evaluated (see **??**).

To literally circunvent the former issue we make use of *Cauchy's Theorem* **??**. For the latter we will apply so-called **pinched weights**.

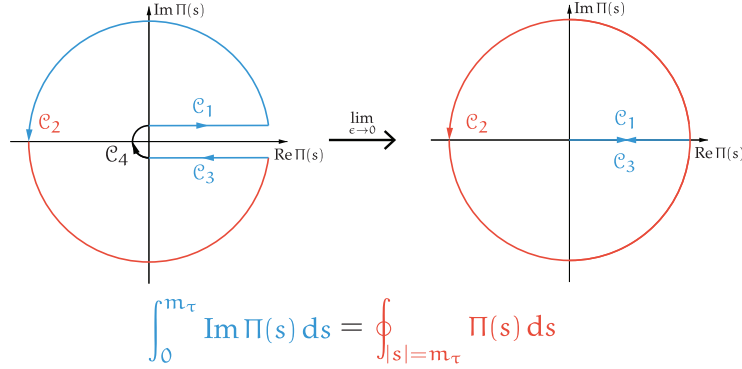$$\int_0^{m_\tau} \operatorname{Im} \Pi(s)\, \mathrm{d}s = \oint_{|s|=m_\tau} \Pi(s)\, \mathrm{d}s$$

Figure 1.2: Visualization of the usage of Cauchy's theorem to transform eq. (1.2) into a closed contour integral over a circle of radius m_τ^2.

1.1 Rescuing pQCD with Cauchy's theorem

We will make use of Cauchy's theorem to rewrite the definite integral of eq. (1.2) into a contour integral over a closed circle with radius m_τ^2. The closed contour consists of four line integrals, which have been visualized in fig. 1.2. Summing over the four line integrals, performing a *analytic continuation* of the two-point correlator $\Pi(s) \rightarrow \Pi(s + i\epsilon)$ and finally taking the limit of $\epsilon \rightarrow 0$ gives us the needed relation between eq. (1.2) and the closed contour:

$$
\begin{aligned}
\oint_{s=m_\tau} \Pi(s) &= \int_0^{m_\tau} \Pi(s+i\epsilon) + \int_{\mathcal{C}_2} \Pi(s)\, \mathrm{d}s + \int_{m_\tau}^0 \Pi(s-i\epsilon)\, \mathrm{d}s + \int_{\mathcal{C}_4} \Pi(s)\, \mathrm{d}s \\
&= \int_0^{m_\tau} \Pi(s+i\epsilon) - \Pi(s-i\epsilon)\, \mathrm{d}s + \int_{\mathcal{C}_2} \Pi(s)\, \mathrm{d}s + \int_{\mathcal{C}_4} \Pi(s)\, \mathrm{d}s \\
&= \int_0^{m_\tau} \Pi(s+i\epsilon) - \overline{\Pi(s+i\epsilon)} + \int_{\mathcal{C}_2} \Pi(s)\, \mathrm{d}s + \int_{\mathcal{C}_4} \Pi(s)\, \mathrm{d}s \\
&\stackrel{\lim \epsilon \to 0}{=} 2i \int_0^{m_\tau} \operatorname{Im} \Pi(s)\, \mathrm{d}s + \oint_{s=m_\tau} \Pi(s)\, \mathrm{d}s
\end{aligned}
\tag{1.13}
$$

where we made use of $\Pi(z) = \overline{\Pi(\bar{z})}$ (due to $\Pi(s)$ is analytic) and $\Pi(z) - \overline{\Pi(z)} = 2i \operatorname{Im} \Pi(z)$. The result can be rewritten in a more intuitive form, which we also visualized in fig. 1.2

$$\int_0^{m_\tau} \Pi(s)\, \mathrm{d}s = \frac{i}{2} \oint_{s=m_\tau} \Pi(s)\, \mathrm{d}s \tag{1.14}$$

Due to the circle-contour we can avoid low energies at which pQCD would break down.

To deal with the latter issue we have to suppress the contributions of the correlator close to the positive real axis, which can be achieved by introducing

4

weight functions, which suppress contributions of the two-point function close to the postive real axis.

Finally combining eq. (1.14) with eq. (1.2) we get

$$R_\tau = 6\pi i \oint_{s=m_\tau} \frac{\mathrm{d}s}{m_\tau^2} \left(1 - \frac{s}{m_\tau^2}\right) \left[\left(1 + 2\frac{s}{m_\tau^2}\right) \Pi^{(T)}(s) + \Pi^{(L)}\right] \qquad (1.15)$$

for the hadronic τ-decay ratio. It is convenient to work with $\Pi^{(T+L)}$, which is connected to the vector/ axial-vector components of the correlator. Thus using eq. (1.10) in eq. (1.15) yields

$$R_\tau = 6\pi i \oint_{|s|=m_\tau} \frac{\mathrm{d}s}{m_\tau^2} \left(1 - \frac{s}{m_\tau^2}\right)^2 \left[\left(1 + 2\frac{s}{m_\tau^2}\right) \Pi^{(L+T)}(s) - \left(\frac{2s}{m_\tau^2}\right) \Pi^{(L)}(s)\right] \qquad (1.16)$$

By introducing Cauchy's theorem we avoided low energies, which could lead to a breakdown of PT. The contour integral obtained is an important result as we are now able to theoretically evaluate the hadronic τ-decay ratio at sufficiently large energy scales ($m_\tau \approx 1.78\,\mathrm{MeV}$) at which $\alpha_s(m_\tau) \approx 0.33$ [**Pich2016**] is large enough to apply perturbation theory and the OPE. Obviously we would benefit from a contour integral over a bigger circumference, but τ-decays are limited by the m_τ. Nevertheless there are promising e^+e^- annihilation data, which yields valuable R-ratio values up to $2\,\mathrm{GeV}$ [**Boito2018**][**Keshavarzi2018**].

1.2 Pinched weights to avoid DVs

We are free to multiply eq. (1.14) by an analytic weight function $\omega(s)$

$$\int_0^{m_\tau} \omega(s)\Pi(s)\,\mathrm{d}s = \frac{i}{2} \oint_{s=m_\tau} \omega(s)\Pi(s)\,\mathrm{d}s. \qquad (1.17)$$

We can use this technique to suppress contributions for the two-point function close to the positive real axis by implementing so called **pinched weights** of the form

$$\omega(s) = (1 - \frac{s}{m_\tau^2})^k, \qquad (1.18)$$

where k is the degree of the pinched weight. The heigher the degree the farther we operate from the critical postivie real axis (see. **??**), which suppresses the effects of duality violations. This pinching of second degree appears quite naturally. If we regard the incluse $\tau - decay$ ratio eq. (1.15), we note that for the transversal component we already have a double pinched weight, the *kinematic weight*

$$\omega_\tau(s) = \left(1 - \frac{s}{m_\tau^2}\right)\left(1 + 2\frac{s}{m_\tau^2}\right). \qquad (1.19)$$

In general it is said that a double pinched weight is sufficient to neglect effects caused by duality violation.
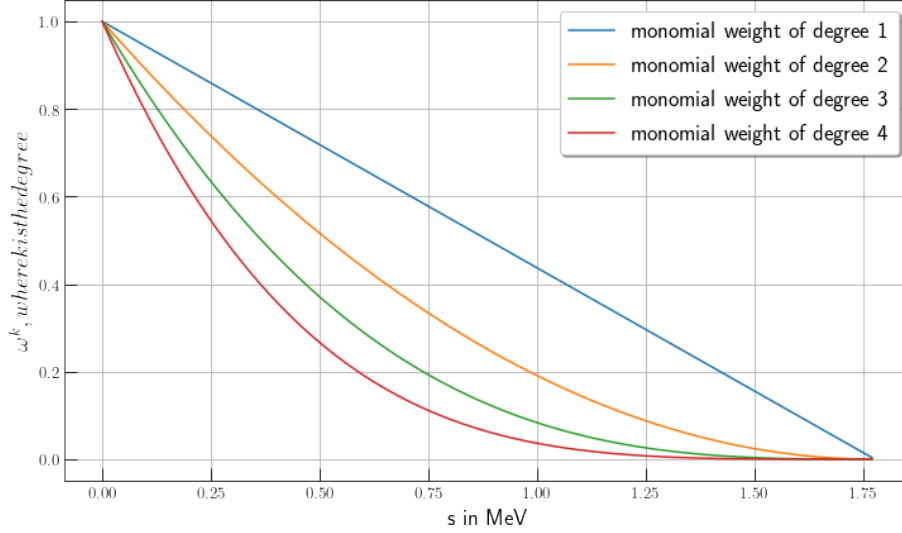
Figure 1.3: Monomial weights $(1 - s/m_\tau^2)^k$ for degrees $1 \to 4$. We can see that weights of heigher pinching decrease faster, which comes in handy if we want to suppress duality violations.

We can also use different weights to control the dimensions of the OPE that contribute. The weights we are using have to be analytic, so that we can make use of Cauchy's theorem. Thus they can be represented as polynomials

$$\omega(x) = \sum_i a_i x^i, \tag{1.20}$$

every contributing monomial is responsible for a dimension of the OPE. Dimensions that are not represented in the weight polynomial do not contribute at all or are very suppressed as we will demonstrate now.

The residue of a monomial x^k is only different from 0 if its power $k = -1$:

$$\oint_C x^k \, \mathrm{d}x = i \int_0^{2\pi} \left(e^{i\theta} \right)^{k+1} \mathrm{d}\theta = \begin{cases} 2\pi i & \text{if } k = -1, \\ 0 & \text{otherwise} \end{cases}. \tag{1.21}$$

Consequently if we exchange the kinematic weight of the incluse ratio eq. (1.1) through a monomial and neglect all terms of no interest to us we can write

$$\begin{aligned}
R(x m_\tau)\big|_{D=0,2,4\dots} &= \oint_{|x|=1} \frac{x^k}{(x m_\tau)^{\frac{D}{2}}} C^D(x m_\tau) \\
&= \frac{1}{(m_\tau)^{\frac{D}{2}}} \oint_{|x|=1} x^{k-D/2} C^D(x m_\tau),
\end{aligned} \tag{1.22}$$

where C^D are the D-dimensional Wilson coefficients. Thus combining eq. (1.21)

monomial:	x^0	x^1	x^2	x^3	x^5	x^6	x^7
dimension:	$D^{(2)}$	$D^{(4)}$	$D^{(6)}$	$D^{(8)}$	$D^{(10)}$	$D^{(12)}$	$D^{(14)}$

Table 1.1: List of monomials and their corresponding "active" dimensions in the OPE.

with eq. (1.22) we see that only Dimension which fulfill

$$k - D/2 = -1 \quad \implies \quad D = 2(k+1) \tag{1.23}$$

contribute to the OPE. For example the polynomial of the kinematic weight is given by

$$(1-x)^2(1+2x) = \underbrace{1}_{D=2} - 3 \underbrace{x^2}_{D=6} + 2 \underbrace{x^3}_{D=8}, \tag{1.24}$$

where we underbraced the monomials and gave the active dimensions. A list of monomomials and their corresponding Dimensions up to dimension 14 can be found in table 1.1. This behaviour enables us to bring out different dimensions of the OPE and suppress contributions of heigher order ($D \geq 10$) for which less is kown.

1.3 RG invariance

The two-point function is not a physical quantity. It does not fulfill the RGE **??** and is thus dependent on the scale μ. We can enhance the inclusive ration eq. (1.1) making use of the **Adler function** defined as:

$$D^{(T+L)}(s) \equiv -s \frac{\mathrm{d}}{\mathrm{d}s} \Pi^{(T+L)}(s), \qquad D^{(L)}(s) \equiv \frac{s}{m_\tau^2} \frac{\mathrm{d}}{\mathrm{d}s}(s\Pi^{(L)}(s)), \tag{1.25}$$

where we have two separate definitions: one for the transversal plus longitudinal contribution and one for solely longitudinal part. The two-point functions can now be replaced with the help of partial integration

$$\int_a^b u(x)V(x)\,\mathrm{d}x = \left[U(x)V(x)\right]_a^b - \int_a^b U(x)v(x)\,\mathrm{d}x. \tag{1.26}$$

We will do the computation for each of the two cases $(T+L)$ and (L) separate. Starting by the transversal plus longitudinal contribution we get:

$$R_\tau^{(1)} = \frac{6\pi i}{m_\tau^2} \oint_{|s|=m_\tau^2} \underbrace{\left(1 - \frac{s}{m_\tau^2}\right)^2 \left(1 + 2\frac{s}{m_\tau^2}\right)}_{=u(x)} \underbrace{\Pi^{(L+T)}(s)}_{=V(x)}$$

$$= \frac{6\pi i}{m_\tau^2} \left\{ \left[-\frac{m_\tau^2}{2}\left(1 - \frac{s}{m_\tau^2}\right)^3 \left(1 + \frac{s}{m_\tau^2}\right) \Pi^{(L+T)}(s) \right]_{|s|=m_\tau^2} \right.$$

$$\left. + \oint_{|s|=m_\tau^2} \underbrace{-\frac{m_\tau^2}{2}\left(1 - \frac{s}{m_\tau^2}\right)^3 \left(1 + \frac{s}{m_\tau^2}\right)}_{=U(x)} \underbrace{\frac{\mathrm{d}}{\mathrm{d}s}\Pi^{(L+T)}(s)}_{=v(x)} \right\} \qquad (1.27)$$

$$= -3\pi i \oint_{|s|=m_\tau^2} \frac{\mathrm{d}s}{s}\left(1 - \frac{s}{m_\tau^2}\right)^3 \left(1 + \frac{s}{m_\tau^2}\right) \frac{\mathrm{d}}{\mathrm{d}s}D^{(L+T)}$$

where we fixed the integration constant to $C = -\frac{m_\tau^2}{2}$ in the second line and left the antiderivatives contained in the squared brackets untouched. If we parametrizing the integral appearing in the expression in the squared brackets we can derive that it vanishes:

$$\left[-\frac{m_\tau^2}{2}\left(1 - e^{-i\phi}\right)^3 \left(1 + e^{-i\phi}\right) \Pi^{(L+T)}(m_\tau^2 e^{-i\phi}) \right]_0^{2\pi} = 0 \qquad (1.28)$$

where $s \to m_\tau^2 e^{-i\phi}$ and $(1 - e^{-i\cdot 0}) = (1 - e^{-i\cdot 2\pi}) = 0$. Repeating the same calculation for the longitudinal part yields

$$R_\tau^{(L)} = \oint_{|s|=m_\tau^2} \mathrm{d}s \left(1 - \frac{s}{m_\tau^2}\right)^2 \left(-\frac{2s}{m_\tau^2}\right) \Pi^{(L)}(s)$$

$$= -4\pi i \oint \frac{\mathrm{d}s}{s}\left(1 - \frac{s}{m_\tau^2}\right)^3 D^{(L)}(s) \qquad (1.29)$$
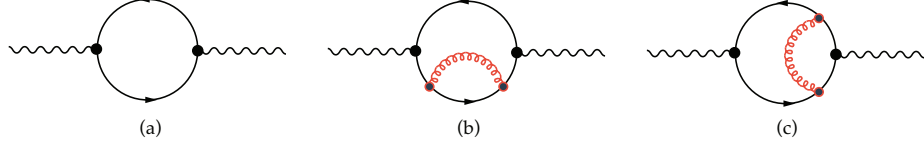
Consequently combining the two parts results in

$$R_\tau = -\pi i \oint_{|s|=m_\tau^2} \frac{\mathrm{d}s}{s}\left(1 - \frac{s}{m_\tau^2}\right)^3 \left[3\left(1 + \frac{s}{m_\tau^2}D^{(L+T)}(s) + 4D^{(L)}(s)\right) \right]. \qquad (1.30)$$

It is convenient to define $x = s/m_\tau^2$ such that we can rewrite the inclusive ratio as

$$R_\tau = -\pi i \oint_{|s|=m_\tau^2} \frac{\mathrm{d}x}{x}(1-x)^3 \left[3(1+x)D^{(L+T)}(m_\tau^2 x) + 4D^{(L)}(m_\tau^2 x) \right]. \qquad (1.31)$$

$$R_{\tau,V/A}^\omega = \frac{N_c}{2}S_{EW}|V_{ud}|^2 \left(1 + \delta_\omega^{(0)} + \delta_\omega^{EW} + \delta_\omega^{DVs} + \sum_{D\leq 2} \delta_{ud,\omega}^{(D)} \right) \qquad (1.32)$$

8

(a)   (b)   (c)

1.4   The perturbative expansion

We will treat the correlator in the chiral limit for which the longitudinal components $\Pi^L(s)$ vanish (see eq. (1.11)) and the axial and vectorial contributions are equal. In the massless case we then can write the vector correlation function $\Pi(s)$ as [**Beneke2008**]:

$$\Pi_V^{T+L}(s) = -\frac{N_c}{12\pi^2} \sum_{n=0}^{\infty} a_\mu^n \sum_{k=0}^{n+1} c_{n,k} L^k \quad \text{with} \quad L \equiv \ln \frac{-s}{\mu^2}. \tag{1.33}$$

The coeffiecient $c_{n,k}$ up to two-loop order can be obtained by Feynman-diagram calculations. add complete calculation E.g. we can compare the zero-loop result of the correlator [**Jamin2006**]

$$\left. \Pi_{\mu\nu}^B(q^2) \right|^{1-loop} = \frac{N_c}{12\pi^2} \left(\frac{1}{\hat{\epsilon}} - \log \frac{(-q^2 - i0)}{\mu^2} + \frac{5}{3} + \mathcal{O}(\epsilon) \right) \tag{1.34}$$

with eq. (1.33) and extract the first two coefficients

$$c_{00} = -\frac{5}{3} \qquad \text{and} \qquad c_{01} = 1, \tag{1.35}$$

where $\Pi_{\mu\nu}^B(q^2)$ is not renormalized[3]

The second loop can also be calculated by diagram techniques resulting in [**Boito2011**]

$$\left. \Pi_V^{(1+0)}(s) \right|^{2-loop} = -\frac{N_c}{12\pi^2} a_\mu \log(\frac{-s}{\mu^2}) + \cdots \tag{1.36}$$

yielding $c_{11} = 1$.

Beginning from three loop diagrams the algebra becomes exausting and one has to use dedicated algorithms to compute the heigher loops. The third loop calculations have been done in the late seventies by [**Chetyrkin1979**, **Dine1979**, **Celmaster1979**]. The four loop evaluation have been completed a little more than ten years later by [**Gorishnii1990**, **Surguladze1990**]. The heighest loop published, that amounts to α_s^4, was published in 2008 [**Baikov2008**] almost 20 years later.

Fixing the number of colors to $N_c = 3$ the missing coefficients up to order

---

[3]The term $1/\hat{\epsilon}$, which is of order 0 in α_s, will be cancelled by renormalization.

four in α_s read:

$$c_{2,1} = \frac{365}{24} - 11\zeta_3 - \left(\frac{11}{12} - \frac{2}{3}\zeta_3\right) N_f$$

$$c_{3,1} = \frac{87029}{288} - \frac{1103}{4}\zeta_3 + \frac{275}{6}\zeta_5$$

$$- \left(\frac{7847}{216} - \frac{262}{9}\zeta_3 + \frac{25}{9}\zeta_5\right) N_f + \left(\frac{151}{162} - \frac{19}{27}\zeta_3\right) N_f^2$$

$$c_{4,1} = \frac{78631453}{20736} - \frac{1704247}{432}\zeta_3 + \frac{4185}{8}\zeta_3^2 + \frac{34165}{96}\zeta_5 - \frac{1995}{16}\zeta_7,$$

(1.37)

where used the flavour number $N_f = 3$ for the last line.

The 6-loop calculation has until today not been achieved, but Beneke und Jamin [**Beneke2008**] used and educated guess to estimate the coefficient

$$c_{5,1} \approx 283 \pm 283.$$

(1.38)

Until now we have given the coefficients $c_{n,k}$ with solely $k = 1$. This is due to the RGE, which relates coefficients with k different than one to the coefficients mentioned above. To make use of the RGE the correlator $\Pi_V^{T+L}(s)$ needs to be a physical quantity, which can be achieved by rewriting it in terms of the Adler function (see. eq. (1.25)) to:

$$D_V^{(T+L)} = -s\frac{\mathrm{d}\Pi_V^{(T+L)}(s)}{\mathrm{d}s} = \frac{N_c}{12\pi^2} \sum_{n=0}^{\infty} a_\mu^n \sum_{k=1}^{n+1} k c_{n,k} L^{k-1},$$

(1.39)

where we used $\mathrm{d}L^k/\mathrm{d}s = k\ln(-s/\mu^2)^{k-1}(-1/\mu^2)$. The Adler-function is physical quantity and has to fulfill the RGE **??**:

$$-\mu\frac{\mathrm{d}}{\mathrm{d}\mu} D_V^{(T+L)} = -\mu\frac{\mathrm{d}}{\mathrm{d}\mu}\left(\frac{\partial}{\partial L}\,\mathrm{d}L + \frac{\partial}{\partial a_s}\,\mathrm{d}a_s\right) D_V^{T+L} = \left(2\frac{\partial}{\partial L} + \beta\frac{\partial}{\partial a_s}\right) D_V^{T+L} = 0,$$

(1.40)

where we defined the β-function in **??** and used $\mathrm{d}L/\mathrm{d}\mu = -2/\mu$. The RGE puts constraints on the $c_{n,k}$-coefficients for different ks, which are not not independent anymore.

For example writing out the sum of the adler function to the second order in α_s yields

$$D(s) = \frac{N_c}{12\pi^2}\left[c_{01} + a_\mu(c_{11} + 2c_{12}L) + a_\mu^2(c_{21} + 2c_{22}L + 3c_{23}L^2)\right].$$

(1.41)

Then inserting eq. (1.41) into the RGE

$$4a_\mu c_{12} + 2a_\mu^2(2c_{22} + 6c_{23}L) + \beta_1 a_\mu^2(c_{11} + 2c_{12}L) + \mathcal{O}(a_\mu^3) = 0$$

(1.42)

lets us compare the coefficients order by order in α_s. At order α_μ only the c_{12} term is present and has to be zero consequently. For $\mathcal{O}(a_\mu^2 L)$ the only c_{23} exists

$(c_{12} = 0)$ and has to vanish as well. Finally at $\mathcal{O}(a)$ we can relate c_{22} with c_{11} resulting in:

$$c_{12} = 0, \quad c_{22} = \frac{\beta_1 c_{11}}{4} \quad \text{and} \quad c_{23} = 0. \tag{1.43}$$

or $D(s)$ to the first order in α_s. Implementing the newly obtained Adler-coefficients we can write out the adler function to the first order:

$$D(s) = \frac{N_c}{12\pi^2} \left[c_{01} + c_{11} a_\mu \left(c_{21} - \frac{1}{2} \beta_1 c_{11} L \right) a_\mu^2 \right] + \mathcal{O}(a_\mu^3). \tag{1.44}$$

We have used the RGE to relate Adler-function coefficients and thus reduce its numbers. But as we will see in the following section the RGE gives us two different choices in the order of the computation of the perturbative contribution to the inclusive τ-decay ratio.

1.4.1 Renormalisation group summation

By making use of the RGE we have to decide about the order of mathematical operations we perform. As the perturbative contribution $\delta^{(0)}$ is independent on the scale μ we are confronted with two choices **fixed-order perturbation theory** (FOPT) or **contour-improved perturbation theory**. Each of them yields a different result and is the main source of error in extracting the strong coupling from τ-decays.

We can write the perturbative contribution $\delta^{(0)}$ to R_τ (see eq. (1.32)) in the chiral limit, such that $D^{(L)}$ vanishes as

$$\delta^{(0)} = \sum_{n=1}^{\infty} a_\mu^n \sum_{k=1}^{n} k c_{n,k} \frac{1}{2\pi i} \oint_{|x|=1} \frac{dx}{x} (1-x)^3 (1+x) \log\left(\frac{-M_\tau^2 x}{\mu^2} \right)^{k-1}, \tag{1.45}$$

where we inserted the expansion of $D_V^{(T+L)}$ eq. (1.25) into R_τ eq. (1.31). Keep in mind that the contributions from the vector and axialvector correlator are identical in the massless case:

$$D^{(T+L)} = D_V^{(T+L)} + D_A^{(T+L)} = 2D_V^{(T+L)}. \tag{1.46}$$

In the following we will explain both the descriptions, starting by FOPT. By using the FOPT prescription we fix $\mu^2 = m_\tau^2$ leading to

$$\delta_{FO}^{(0)} = \sum_{n=1}^{\infty} a(m_\tau^2)^n \sum_{k=1}^{n} k c_{n,k} J_{k-1} \tag{1.47}$$

where the contour integrals J_l are defined by

$$J_l \equiv \frac{1}{2\pi i} \oint_{|x|=1} \frac{dx}{x} (1-x)^3 (1+x) \log^l(-x). \tag{1.48}$$

11

The integrals J_l up to order α_s^4 are given by [**Beneke2008**]:

$$J_0 = 1, \quad J_1 = -\frac{19}{12} \quad J_2 = \frac{265}{72} - \frac{1}{3}\pi^2, \quad J_3 = -\frac{3355}{288} + \frac{19}{12}\pi^2. \tag{1.49}$$

Using FOPT the strong coupling $a(\mu)$, which runs with the scale μ, is fixed at $a(m_\tau^2)$ and can be taken out of the closed-contour integral. Thus we solely to integrate over the logarithms $\log(-s/m_\tau^2)$.

Using CIPT we can sum the logarithms by setting the scale to $\mu^2 = -m_\tau^2 x$ in eq. (1.45), resulting in:

$$\delta_{CI}^{(0)} = \sum_{n=1}^{\infty} c_{n,1} J_n^a(m_\tau^2), \tag{1.50}$$

where the contour integrals J_l are defined by

$$J_n^a(m_\tau^2) \equiv \frac{1}{2\pi i} \oint_{|x|=1} \frac{\mathrm{d}x}{x}(1-x)^3(1+x)a^n(-m_\tau^2 x). \tag{1.51}$$

All logarithms vanish except the ones for $k = 1$:

$$\log(1)^{k-1} = \begin{cases} 1 & \text{if } k = 1, \\ 0 & k \neq 1 \end{cases} \tag{1.52}$$

which selectes adler function coefficients $c_{n,1}$ with a fixed $k = 1$. Handling the logarithms left us with the integration of $\alpha_s(-m_\tau^2 x)$ over the closed-contour $\oint_{|x|=1}$, which now depends on the integration variable x. In general we have to decide if we want to perform a contour integration with a constant coupling constant and variable logarithms (FOPT) or "constant logarithms" and a running coupling (CIPT).

To emphasize the differences in both approaches we can calculate the perturbative contribution $\delta^{(0)}$ to R_τ for the two different prescriptions yielding [**Beneke2008**]

$$\begin{array}{ccccc} \alpha_s^2 & \alpha_s^2 & \alpha_s^3 & \alpha_s^4 & \alpha_s^5 \end{array}$$

$$\delta_{FO}^{(0)} = 0.1082 + 0.0609 + 0.0334 + 0.0174(+0.0088) = 0.2200(0.2288) \tag{1.53}$$

$$\delta_{CI}^{(0)} = 0.1479 + 0.0297 + 0.0122 + 0.0086(+0.0038) = 0.1984(0.2021). \tag{1.54}$$

The series indicate, that CIPT converges faster and that both series aproach a different value. This discrepancy represents currently the biggest theoretical uncertainity while extracting the strong coupling α_s.

As today we do not know if FOPT or CIPT is the correct approach of measuring α_s. Therefore there are currently three ways of stating results:

- Quoting the average of both results.

- Quoting the CIPT result.

- Quoting the FOPT result.

We follow the approach of Beneke and Jamin [**Benke2008**] who have shown advantages of FOPT over CIPT.

1.5   Non-Perturbative OPE Contribution

The perturbative contribution to the Sum-Rule, that we have seen so far, is the dominant one. With

$$
\begin{aligned}
R_\tau^{FOPT} &= \\
R_\tau^{CIPT} &=
\end{aligned}
\tag{1.55}
$$

The NP vs perturbative contributions can be varied by choosen different weights than ω_τ.

1.5.1   Dimension four

For the OPE contributions of dimension four we have to take into account the terms with masses to the fourth power m^4, the quark condensate multiplied by a mass $m\langle\bar{q}\,q\rangle$ and the glucon condensate $\langle GG\rangle$. The resulting expression can be taken from the appendix of [**Pich1999**], yielding:

$$
D_{ij}^{(L+T)}(s)\Big|_{D=4} = \frac{1}{s^2}\sum_n \Omega^{(1+0)}(s/\mu^2)a^n,
\tag{1.56}
$$

where

$$
\begin{aligned}
\Omega_n^{(1+0)}(s/\mu^2) ={}& \frac{1}{6}\langle aGG\rangle p_n^{(L+T)}(s/\mu^2) + \sum_k m_k\langle\bar{q}_k q_k\rangle r_n^{(L+T)}(s/\mu^2) \\[4pt]
&+ 2\langle m_i\bar{q}_i q_i + m_j\bar{q}_j q_j\rangle q_n^{(L+T)}(s/\mu^2) \pm \frac{8}{3}\langle m_j\bar{q}_i q_i + m_i\bar{q}_j q_j\rangle t_n^{(L+T)} \\[4pt]
&- \frac{3}{\pi^2}(m_i^4 + m_j^4)h_n^{(L+T)}(s/\mu^2) \mp \frac{5}{\pi^2}m_i m_j(m_i^2 + m_j^2)k_n^{(L+T)}(s/\mu^2) \\[4pt]
&+ \frac{3}{\pi^2}m_i^2 m_j^2 g_n^{(L+T)}(s/\mu^2) + \sum_k m_k^4 j_n^{(L+T)}(s/\mu^2) + 2\sum_{k\neq l} m_k^2 m_l^2 u_n^{(L+T)}(s/\mu^2)
\end{aligned}
\tag{1.57}
$$

The perturbative expansion coefficients are known to $\mathcal{O}(a^2)$ for the condensate contributions,

$$
\begin{aligned}
p_0^{(L+T)} &= 0, & p_1^{(L+T)} &= 1, & p_2^{(L+T)} &= \tfrac{7}{6}, \\
r_0^{(L+T)} &= 0, & r_1^{(L+T)} &= 0, & r_2^{(L+T)} &= -\tfrac{5}{3} + \tfrac{8}{3}\zeta_3 - \tfrac{2}{3}\log(s/\mu^2), \\
q_0^{(L+T)} &= 1, & q_1^{(L+T)} &= -1, & q_2^{(L+T)} &= -\tfrac{131}{24} + \tfrac{9}{4}\log(s/\mu^2) \\
t_0^{(L+T)} &= 0 & t_1^{(L+T)} &= 1, & t_2^{(L+T)} &= \tfrac{17}{2} + \tfrac{9}{2}\log(s/\mu^2).
\end{aligned}
\tag{1.58}
$$

while the m^4 terms have been only computed to $\mathcal{O}(a)$

$$
\begin{aligned}
h_0^{(L+T)} &= 1 - 1/2\log(s/\mu^2), & h_1^{(L+T)} &= \tfrac{25}{4} - 2\zeta_3 - \tfrac{25}{6}\log(s/\mu^2) - 2\log(s/\mu^2)^2, \\
k_0^{(L+T)} &= 0, & k_1^{(L+T)} &= 1 - \tfrac{2}{5}\log(s/\mu^2), \\
g_0^{(L+T)} &= 1, & g_1^{(L+T)} &= \tfrac{94}{9} - \tfrac{4}{3}\zeta_3 - 4\log(s/\mu^2), \\
j_0^{(L+T)} &= 0, & j_1^{(L+T)} &= 0, \\
u_0^{(L+T)} &= 0, & u_2^{(L+T)} &= 0.
\end{aligned}
\tag{1.59}
$$

1.5.2 Dimension six and eight

Our application of dimension six contributions is founded in [**Braaten1991**] and has previously been calculated beyond leading order by [**Lanin1986**]. The operators appearing are the masses to the power six m^6, the four-quark condensates $\langle \bar{q}\, q \bar{q}\, q \rangle$, the three-gluon condensates $\langle g^3 G^3 \rangle$ and lower dimensional condensates multiplies by the corresponding masses, such that in total the mass dimension of the operator will be six. As there are too many parameters to be fitted with experimental data we have to omit some of them, starting with the three-gluon condensate, which does not contribute at leading order. The four-quark condensates known up to $\mathcal{O}(a^2)$, but we will make use of the *vacuum saturation approach* [**Beneke2008**, **Braaten1991**, **Shifman1978**] to express them in quark, anti-quark condensates $\langle q \bar{q} \rangle$. In our work we take the simplest approach possible: Introducing an effective dimension six coefficient $\rho_{V/A}^{(6)}$ divided by the appropiate power in s

$$D_{ij,V/A}^{(1+0)}\Big|_{D=6} = 0.03 \frac{\rho_{V/A}^{(6)}}{s^3} \tag{1.60}$$

As for the dimension eigth contribution the situation is not better than the dimension six one we keep the simplest approach, leading to

$$D_{ij,V/A}^{(1+0)}\Big|_{D=8} = 0.04 \frac{\rho_{V/A}^{(8)}}{s^4}. \tag{1.61}$$

1.5.3 Duality Violations

1.6 Experiment

The τ-decay data we use to perform our QCD-analysis is from the **ALEPH** experiment. The ALEPH experiment was located at the large-electron-positron (LEP) collider at CERN laboratory in Geneva. LEP started producing particles in 1989 and was replaced in the late 90s by the large-hadron-collider, which makes use of the same tunnel of 27km circumference. The data produced within the experiment is still maintained by former ALEPH group members under led by M. Davier, which have performed regular updates on the data-sets [**Davier2013**, **Davier2008**, **Schael2005**].

The measured spectral functions for the Aleph data are defined in [**Davier2007**] and given for the transversal and longitudinal components separatly:

$$\rho_{V/A}^{(T)}(s) = \frac{m_\tau^2}{12\left|V_{ud}^2\right| S_{EW}} \frac{\mathcal{B}(\tau^- \to V^-/A^- \nu_\tau)}{\mathcal{B}(\tau^- \to e^- \overline{\nu}_e \nu_\tau)}$$
$$\times \frac{\mathrm{d}N_{V/A}}{N_{V/A}\,\mathrm{d}s} \left[\left(1 - \frac{s}{m_\tau^2}\right)^2 \left(1 + \frac{2s}{m_\tau^2}\right)\right]^{-1} \tag{1.62}$$
$$\rho_A^{(L)}(s) = \frac{m_\tau^2}{12\left|V_{ud}^2 S_{EW}\right|} \frac{\mathcal{B}(\tau^- \to \pi^-(K^-)\nu_\tau)}{\mathcal{B}(\tau^- \to e^- \overline{\nu}_e \nu_\tau)} \times \frac{\mathrm{d}N_A}{N_A\,\mathrm{d}s} \left(1 - \frac{s}{m_\tau^2}\right)^{-2}.$$

$$\mathcal{B}_e = \dots \tag{1.63}$$

$$R_{\tau,V/A} = \frac{B_{V/A,\tau}}{B_e} \tag{1.64}$$

The data relies on a separation into vector and axial-vector channels. In the case of the Pions this can be achieved via counting. The vector channel is characterized by a negative parity, whereas the axial-vector channel has positive parity. A quark has by definition positive parity, thus an anti-quark has a negative parity. A meson, like the Pion particle, is a composite particle consiting of an quark an anti-quark. Consequently a single Pion carries negative parity, an even number of Pions carries positive parity and an odd number of Pions carries negative parity:

$$n \times \pi = \begin{cases} \text{vector} & \text{if } n \text{ is even,} \\ \text{axial-vector} & \text{otherwise} \end{cases}. \tag{1.65}$$

The contributions to the vector and axial channel can be seen in figure. The dominant modes in the vector case are [**Davier2006**] $\tau^- \to \pi^- \pi^0 \nu_\tau$ and the $\tau^- \to \pi^- \pi^- \pi^+ \pi^0 \nu_\tau$. The first of these is produced by the $\rho(770)$ meson, which in contrary to the pions carries angular momentum of one, which is also clearly visible as peak around $770\,\text{GeV}$ in figure vector. The dominant modes in the axial-vector case are $\tau^- \to \pi^- \nu_\tau$, $\tau^- \to \pi^- \pi^0 \pi^0 \nu_\tau$ and $\tau^- \to \pi^- \pi^- \pi^+ \nu_\tau$. Here the three pion final states stem from the a_1^--meson, which is also clearly visible as a peak in figure.

wavy =¿ DV OPE cannot reproduce suppressed in VpA regions below 1.5 GeV can still not be applied

The different inclusive τ-decay ratios are then given by

$$R_{\tau,V} = \dots \tag{1.66}$$

1.7 Fits

1.7.1 Kinematic weight: $\omega(x) = (1-x)^2(1+2x)$

The kinematic weight $\omega(x) = (1-x)^2(1+2x)$ is the natural appearing weight carried by the eq. (1.1). Its polinomial contains terms proportional to x^2 and x^3 which makes it sensitive to $D = 6$ and $D = 8$ contributions from the OPE. Consequently we fitted the strong coupling $\alpha_s(m_\tau^2)$ and the OPE coefficients for dimension six and eight. The fits have been performed within the framework of FOPT for different numbers of s_0. The momentum sets are characterized by its lowest energy s_{min}. We fitted values up to $1.5\,\text{GeV}$, as including more moments causes problems with the convergence of our fitting routine. This is due to their heigh correlation which has been plotted in correlation plot?? Going to lower energies also bares the risk to be affected by the $\rho(770)$ and a_1 peaks in the
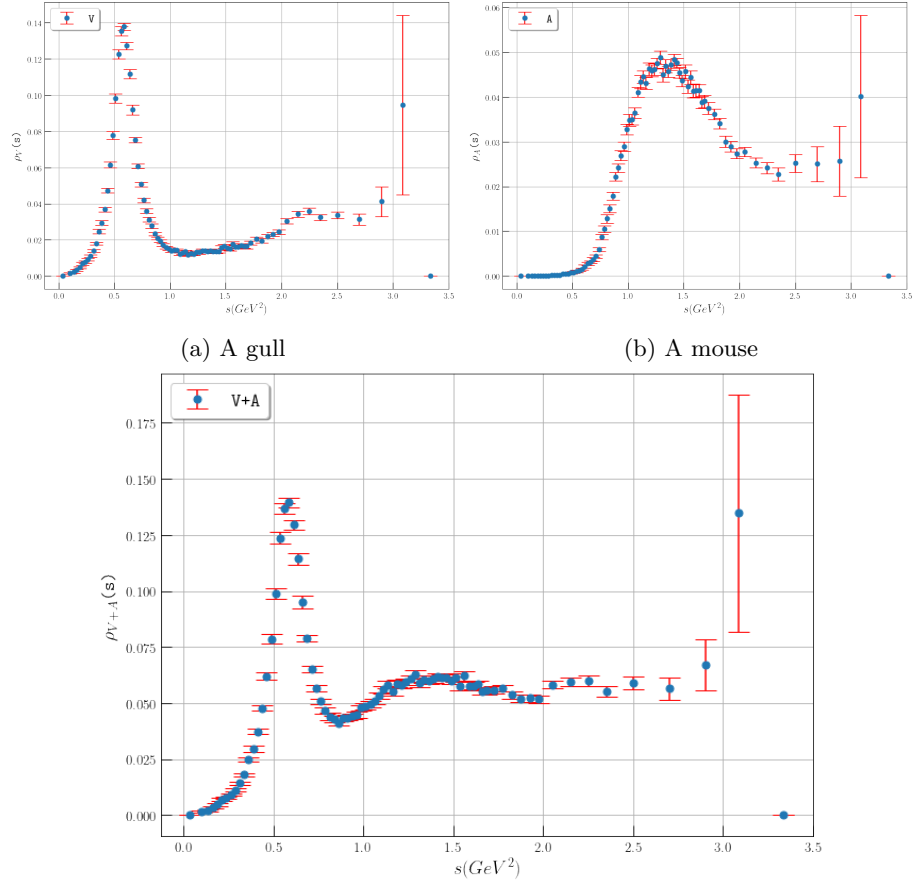
(a) A gull

(b) A mouse

Figure 1.4: Pictures of animals

vector and axial-vector spectral function. We have given all of our fit values in table 1.2 and fig. 1.5.

s_{min}	#s_0s	$\alpha_s(m_\tau^2)$	c_6	c_8	χ^2/dof
1.500	23	0.3255(13)	-0.441(10)	-0.2909(34)	2.00
1.525	22	0.3255(18)	-0.440(36)	-0.288(45)	2.10
1.550	21	0.3265(16)	-0.478(36)	-0.343(50)	1.81
1.575	20	0.3269(22)	-0.493(47)	-0.365(58)	1.86
1.600	19	0.3272(23)	-0.506(51)	-0.384(64)	1.94
1.625	18	0.3284(24)	-0.540(53)	-0.433(68)	1.788
1.650	17	0.3283(24)	-0.550(57)	-0.448(74)	1.90
1.675	16	0.3284(24)	-0.549(57)	-0.448(79)	2.04
1.700	15	0.3281(24)	-0.538(63)	-0.430(87)	2.19
1.750	14	0.3291(26)	-0.581(71)	-0.50(10)	2.21
1.800	13	0.3293(27)	-0.589(77)	-0.51(11)	2.43
1.850	12	0.3281(28)	-0.537(85)	-0.42(13)	2.5
1.900	11	0.3272(29)	-0.493(93)	-0.35(15)	2.65
1.950	10	0.3232(32)	-0.31(11)	-0.01(18)	1.13
2.000	9	0.3234(34)	-0.32(12)	-0.03(21)	1.31
2.100	8	0.3256(38)	-0.43(15)	-0.25(28)	1.30
2.200	7	0.3308(44)	-0.72(20)	-0.85(38)	0.19
2.300	6	0.3304(52)	-0.69(25)	-0.80(50)	0.25
2.400	5	0.3339(70)	-0.91(39)	-1.29(83)	0.10
2.600	4	0.3398(15)	-1.3(1.0)	-2.3(2.5)	0.01

Table 1.2: Table of our fitting values of $\alpha_s(m_\tau^2), c_6$ and c_8 for the kinematic weight $\omega(x) = (1-x)^2(1+2x)$ using FOPT ordered by increasing s_{min}. The errors are given in parenthesis after the observed value.
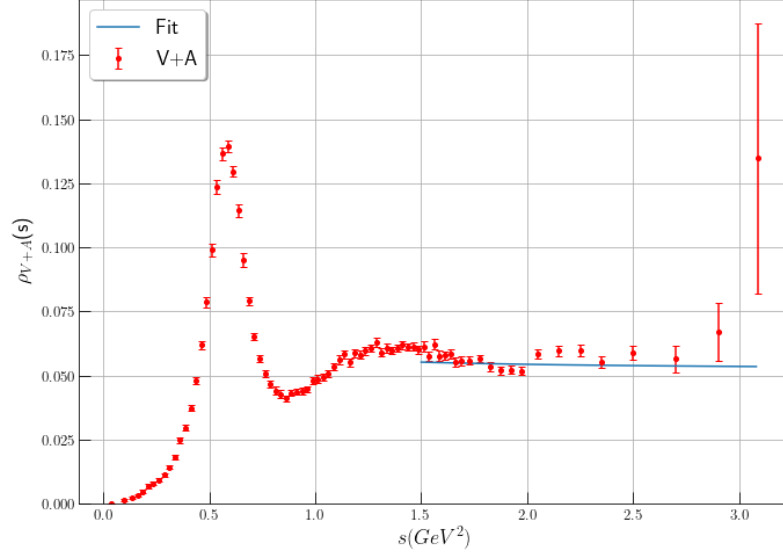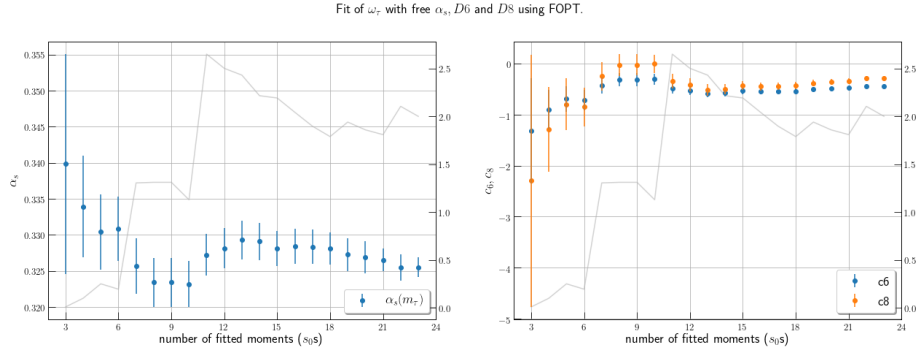
Figure 1.6: test

Figure 1.5: Fitting values of $\alpha_s(m_\tau^2), c_6$ and c_8 for the kinematic weight $\omega(x) = (1-x)^2(1+2x)$ using FOPT for different s_{min}. The left graph plots $\alpha_s(m_\tau^2)$ for different numbers of used s_0s. The right plot contains the dimension six and eight contributions to the OPE. Both plots have in gray the χ^2 per degree of freedom (dof).

The fits are very stable as we can see in table 1.2 and **??**. The obtained values for $\alpha_s(m_\tau^2)$ are very consitent and vary little. Their standard derivation is of order 10^{-4}. Furthermore the errors of the strong coupling are small. The

Fit of ω_τ with fixed $\alpha_s = 0.3179$, $D6$ and $D8$ using FOPT.
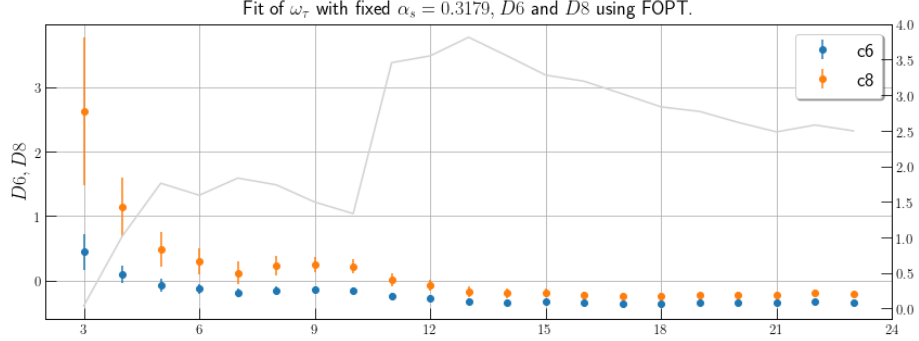
averaged relative error is as small as 1% for all of the fits. The χ^2 per **degree of freedom** (dof) is good and has its best value of 1.13 for $8 - s_0$s moments for $s_{min} = 1.95$. All of the values have a converging OPE, meaning that the values of c_8 are of the order 10 smaller than values of c_6.

D6, D8 stability

1.7.2 Cubic weight: $\omega(x) = (1 - x)^3(1 + 3x)$

s_{min}	#s_0s	$\alpha_s(m_\tau^2)$	c_6	c_8	c_{10}	χ^2/dof
1.800	13	0.3305(37)	-0.493(76)	-0.48(12)	-0.66(20)	2.99
1.850	12	0.3303(37)	-0.482(68)	-0.456(100)	-0.62(17)	3.35
1.900	11	0.3249(29)	-0.280(20)	-0.088(21)	0.088(55)	1.58
1.950	10	0.3237(26)	-0.232(25)	0.005(42)	0.275(93)	1.67
2.000	9	0.3228(26)	-0.196(27)	0.075(28)	0.420(56)	1.96
2.100	8	0.3302(40)	-0.52(11)	-0.58(22)	-1.00(45)	0.43
2.200	7	0.3312(43)	-0.56(12)	-0.68(23)	-1.23(50)	0.55
2.300	6	0.336(11)	-0.78(47)	-1.17(98)	-2.38(22)	0.29
2.400	5	0.3330(96)	-0.63(47)	-0.82(10)	-1.51(26)	0.48

Table 1.3: Table of our fitting values of $\alpha_s(m_\tau^2), c_6$, c_8 and c_{10} for the cubic weight $\omega(x) = (1 - x)^3(1 + 3x)$ using FOPT ordered by increasing s_{min}. The errors are given in parenthesis after the observed value.

19

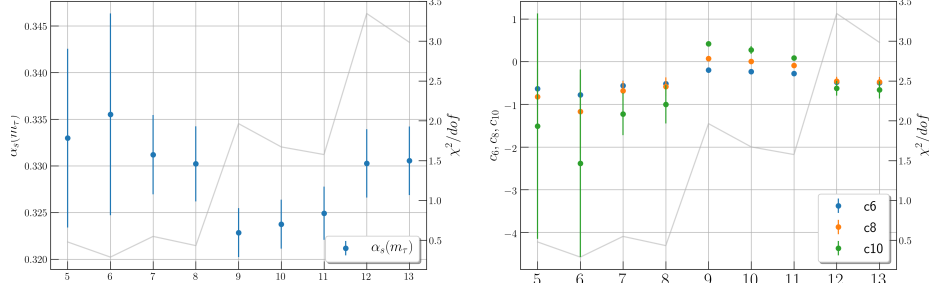### 1.7.3   Quartic weight: $\omega(x) = (1-x)^4(1+4x)$

s_{min}	$\#s_0$s	$\alpha_s(m_\tau^2)$	c_6	c_8	c_{10}	χ^2/dof
1950	10	0.3308(12)	-0.3499(62)	-0.2453(55)	-0.1779(45)	1.21
2000	9	0.3290(99)	-0.3030(44)	-0.1874(30)	-0.1207(44)	0.54
2100	8	0.3278(12)	-0.2749(48)	-0.1515(28)	-0.0841(47)	0.48
2200	7	0.3286(28)	-0.296(40)	-0.181(48)	-0.117(49)	0.51
2300	6	0.3304(30)	-0.352(54)	-0.262(71)	-0.210(79)	0.41

Table 1.4: Table of our fitting values of $\alpha_s(m_\tau^2), c_6$, c_8 and c_{10} for the quartic weight $\omega(x) = (1-x)^4(1+4x)$ using FOPT ordered by increasing s_{min}. The errors are given in parenthesis after the observed value.

1.7.4 Single pinched third power monomial: $\omega(x) = 1 - x^3$

s_{min}	$\#s_0$s	$\alpha_s(m_\tau^2)$	c_8	χ^2/dof
1.500	23	0.3160(28)	-0.523(65)	2.4
1.525	22	0.3171(28)	-0.578(70)	2.3
1.550	21	0.3173(29)	-0.587(76)	2.42
1.575	20	0.3187(29)	-0.667(82)	2.08
1.600	19	0.3189(30)	-0.679(87)	2.19
1.625	18	0.3195(30)	-0.719(94)	2.24
1.650	17	0.3205(30)	-0.783(99)	2.1
1.675	16	0.3204(31)	-0.77(11)	2.24
1.700	15	0.3206(31)	-0.79(11)	2.39
1.750	14	0.3202(32)	-0.76(13)	2.57
1.800	13	0.3217(33)	-0.88(14)	2.41
1.850	12	0.3202(35)	-0.75(16)	2.4
1.900	11	0.3202(36)	-0.75(18)	2.67
1.950	10	0.3161(38)	-0.40(20)	1.46
2.000	9	0.3148(39)	-0.28(22)	1.47
2.100	8	0.3147(44)	-0.27(29)	1.71
2.200	7	0.3214(49)	-1.01(39)	0.41
2.300	6	0.3227(57)	-1.18(54)	0.46
2.400	5	0.3257(67)	-1.58(74)	0.39
2.600	4	0.325(10)	-1.54(1.53)	0.58
2.800	3	0.326(21)	-1.69(4.03)	1.17

Table 1.5: Table of our fitting values of $\alpha_s(m_\tau^2)$, and c_8 for the single pinched fourth power monomial weight $\omega(x) = 1 - x^3$ using FOPT ordered by increasing s_{min}. The errors are given in parenthesis after the observed value.

1.7.5   Single pinched fourth power monomial: $\omega(x) = 1 - x^4$

s_{min}	$\#s_0$s	$\alpha_s(m_\tau^2)$	c_{10}	χ^2/dof
1.500	23	0.3144(27)	-0.572(80)	2.44
1.525	22	0.3155(27)	-0.655(90)	2.34
1.550	21	0.3157(28)	-0.671(99)	2.45
1.575	20	0.3171(28)	-0.80(11)	2.1
1.600	19	0.3173(29)	-0.82(12)	2.21
1.625	18	0.3180(29)	-0.88(13)	2.24
1.650	17	0.3190(30)	-0.98(14)	2.1
1.675	16	0.3189(30)	-0.97(15)	2.24
1.700	15	0.3192(30)	-1.00(16)	2.39
1.750	14	0.3188(32)	-0.96(19)	2.58
1.800	13	0.3204(32)	-1.17(21)	2.39
1.850	12	0.3190(34)	-0.95(26)	2.4
1.900	11	0.3189(35)	-0.94(29)	2.67
1.950	10	0.3149(37)	-0.31(34)	1.47
2.000	9	0.3137(39)	-0.08(39)	1.5
2.100	8	0.3136(43)	-0.07(54)	1.75
2.200	7	0.3203(48)	-1.64(77)	0.42
2.300	6	0.3216(56)	-2.01(1.13)	0.47
2.400	5	0.3247(66)	-2.98(1.62)	0.39
2.600	4	0.324(10)	-2.86(3.69)	0.58
2.800	3	0.325(20)	-3.43(10.74)	1.17

Table 1.6: Table of our fitting values of $\alpha_s(m_\tau^2)$ and c_{10} for the single pinched fourth power monomial weight $\omega(x) = 1 - x^4$ using FOPT ordered by increasing s_{min}. The errors are given in parenthesis after the observed value.

1.7.6   Optimal Moments

$$\omega^{(n,m)}(x) = (1-x)^n \sum_{k=0}^{m}(k+1)x^k \tag{1.67}$$

$$\omega(x) = (1-x)^3$$

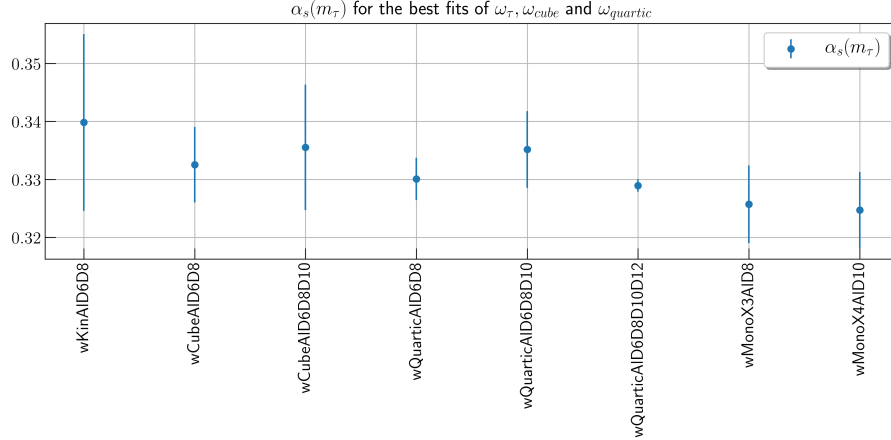| s_{min}	#s_0s	$\alpha_s(m_\tau^2)$	$aGGInv$	c_6	χ^2/dof
1.500	23	0.3276(13)	-0.0077(10)	0.330(35)	2.62
1.525	22	0.3278(14)	-0.0078(10)	0.330(38)	2.75
1.550	21	0.3299(16)	-0.0092(12)	0.333(37)	2.31
1.575	20	0.3308(25)	-0.0098(13)	0.334(47)	2.32
1.600	19	0.3317(28)	-0.0105(14)	0.335(54)	2.38
1.625	18	0.3336(21)	-0.0118(14)	0.340(46)	2.09
1.650	17	0.3345(34)	-0.0124(17)	0.342(62)	2.15
1.675	16	0.3349(25)	-0.0127(15)	0.342(51)	2.28
1.700	15	0.3348(33)	-0.0126(18)	0.342(58)	2.47
1.750	14	0.3372(43)	-0.0145(23)	0.341(71)	2.34
1.800	13	0.3378(31)	-0.0149(20)	0.339(58)	2.54
1.850	12	0.3365(38)	-0.0138(25)	0.346(60)	2.72
1.900	11	0.3355(40)	-0.0128(28)	0.354(59)	2.97
1.950	10	0.3296(47)	-0.0073(34)	0.418(58)	1.57
2.000	9	0.3299(50)	-0.0076(39)	0.414(64)	1.83
2.100	8	0.3331(54)	-0.0108(45)	0.361(76)	1.9
2.200	7	0.3401(57)	-0.0185(52)	0.220(88)	0.73
2.300	6	0.3383(68)	-0.0165(67)	0.26(12)	0.89
2.400	5	0.3450(93)	-0.0243(99)	0.10(17)	0.71
2.600	4	0.337(16)	-0.014(18)	0.36(45)	0.98

Table 1.7: Table of our fitting values of $\alpha_s(m_\tau^2)$, $aGGInv$ and c_6 for the triple pinched optimal weight $\omega^{(3,0)}(x) = (1-x)^3$ using FOPT ordered by increasing s_{min}. The errors are given in parenthesis after the observed value.
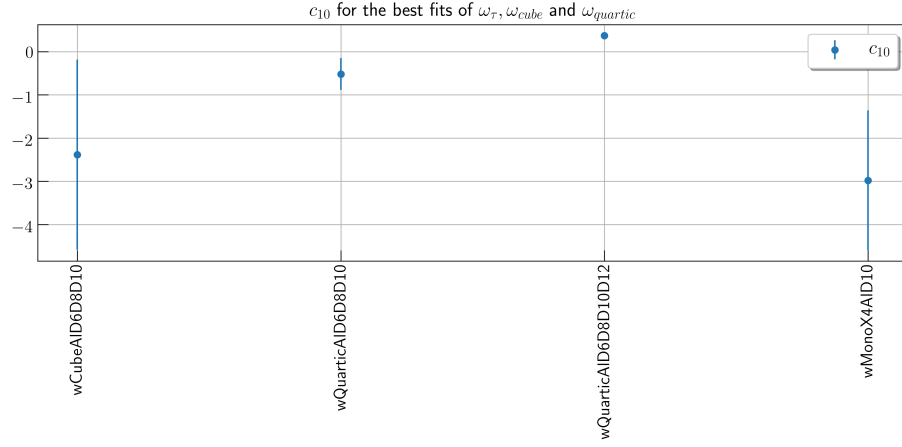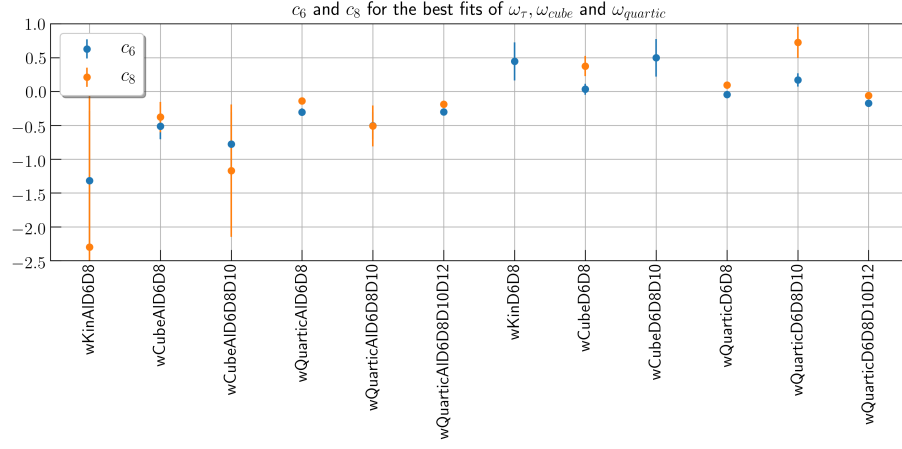
$$\omega(x) = (1-x)^4$$

s_{min}	$\#s_0$s	$\alpha_s(m_\tau^2)$	$aGGInv$	c_6	c_8	χ^2/dof
1.900	11	0.34283(71)	-0.01404(44)	-0.1037(23)	-0.534(20)	1.52
1.950	10	0.34154(73)	-0.01234(95)	-0.050(28)	-0.389(53)	1.42
2.000	9	0.3399(14)	-0.0105(22)	0.002(79)	-0.24(15)	1.59
2.100	8	0.3480(20)	-0.0194(22)	-0.265(72)	-1.03(19)	0.31
2.200	7	0.3483(47)	-0.0197(49)	-0.27(15)	-1.05(43)	0.41
2.300	6	0.3522(53)	-0.0242(60)	-0.42(19)	-1.51(58)	0.29
2.400	5	0.348(17)	-0.019(18)	-0.25(56)	-0.95(17)	0.39

Table 1.8: Table of our fitting values of $\alpha_s(m_\tau^2), aGGInv, c_6$ and c_8 for the optimal weight $\omega^{(4,0)}(x) = (1-x)^4$ using FOPT ordered by increasing s_{min}. The errors are given in parenthesis after the observed value.

1.7.7 Comparison

c_6 and c_8 for the best fits of $\omega_\tau, \omega_{cube}$ and $\omega_{quartic}$

c_{10} for the best fits of $\omega_\tau, \omega_{cube}$ and $\omega_{quartic}$

1.7.8   Toni Pich 2006

4. ALEPH determination

Toni built moments with five different weights:

$$\omega_{kl(x)} = (1-x)^{2+k} x^l (1+x) \quad \text{with} \quad (k,l) = (0,0),(1,0),(1,1),(1,2),(1,3) \tag{1.68}$$

He always fitted weight combinations, which we do not include.

25

5. Optimal moments

Used single moments

$$\omega^{(n,m)}(x) = (1-x)^n \sum_{k=0}^{n} (k+1)x^k \quad \text{with} \quad (n,m) = (1,0),(1,1),(1,2),(1,3),(1,4),(1,5),(2,0),(2,1),(2,2),(2,3)$$

(1.69)

but omitted NPT corrections! He fitted the kinematic weight with free α_s for $\omega(x)^{(2,1)}$. Later on he uses combined fits which is not in our interest. It is called optimal moments, because n stands for the pinching factor, which suppresses DV!

6. Including information from the s_0 dependence

Pich fits $A^{(2,0)}, A^{(2,1)}$ and $A^{(2,2)}$ separately for $s_{min} = 2\,\text{GeV}$. The corresponding weights with fitted OPE dimensions are given by:

$$\omega^{(2,0)} = (1-x)^2 \quad c_4, c_6 \tag{1.70}$$

$$\omega^{(2,1)} = \omega_\tau \quad c_6, c_8 \tag{1.71}$$

$$\omega^{(2,2)} = (1-x)^2(1+2x+x^2) = (x^2-1)^2 \quad c_8, c_{10} \tag{1.72}$$

Thus we can compare our results from the kinematic weight with his results and furthermore add $(1-x)^2$ to our fitting list?

Alpha is comparable, which just have a bigger error. For D6 and D8 we have to compare our definition of c_6, c_8 with his.